applied sciences

MDPI

Communication

Capillary Rise in Layered Soils

Zhenhua Zhao [1,2], Zhenjiang Luo [1,2,*], Hongjie Sun [1,2], Haitao Li [1,2], Qiang Liu [3] and Haiyan Liu [3]

[1] 801 Institute of Hydrogeology and Engineering Geology, Jinan 250000, China
[2] Shandong Engineering Research Center for Environmental Protection and Remediation on Groundwater, Jinan 250000, China
[3] College of Earth Science and Engineering, Shandong University of Science and Technology, Jinan 250000, China
* Correspondence: luozhenjiang89@gmail.com

Abstract: Capillary rise tests were conducted on soil columns containing of three layers of sandy soils with coarser over finer over coarser sandy soil to investigate the effect of the relatively finer soil interlayer. The capillary rise height, rate, and water distribution were observed in laboratory tests of four layered soil columns, with two homogeneous (without the interlayer) soil columns serving as the controls. The final maximum height of the capillary rise in the soil column with the interlayer was larger than that of the column without the interlayer when the interlayer was laid around the water entry value of the underlying soil. The water content was not continuous in the entire soil profile with the interlayer, and a small matric suction gap was observed in the relatively fine soil between the soil column with and without the interlayer.

Keywords: unsaturated soil; capillary rise; layered soil; water entry value

check for updates

Citation: Zhao, Z.; Luo, Z.; Sun, H.; Li, H.; Liu, Q.; Liu, H. Capillary Rise in Layered Soils. *Appl. Sci.* **2023**, *13*, 3374. https://doi.org/10.3390/app13063374

Academic Editors: Bing Bai, Daniel Dias, Angeles Sanroman Braga and Tiago Miranda

Received: 10 August 2022
Revised: 7 January 2023
Accepted: 16 January 2023
Published: 7 March 2023

Copyright: © 2023 by the authors. Licensee MDPI, Basel, Switzerland. This article is an open access article distributed under the terms and conditions of the Creative Commons Attribution (CC BY) license (https://creativecommons.org/licenses/by/4.0/).

1. Introduction

The capillary rise of water is an important phenomenon, as it can enhance the soil freezing, thawing, and settlements of buildings. It can also cause damage to both concrete and steel if the water contains erosive ions, or influences the water balance and management in irrigated areas with shallow groundwater tables [1] To evaluate the water capillarity of the soil, the maximum capillary height, the water content profile, and the rate of capillary rise are the three keys. Hird and Bolton [2] used the column test, which controlled the relative air humidity above sample surface and the temperature of the entire sample, to discuss the capillary height. Polansky and Kaya [3] proposed a model to predict the overall behavior of the capillary rise dynamics in a heated capillary tube. Liu et al. [4] proposed a new theoretical solution for quick and easy estimation of the maximum height of the capillary rise in homogeneous soil. However, the soil deposit is usually layered. Soil texture has a decisive effect on the hydraulic properties of soil, such as unsaturated hydraulic conductivities ($k(h)$), soil water retention curve (SWRC), field capacity, air entry value, and capillary rise height and rate [5]. Typically, the finer the soil texture is, the greater the porosity, the water retention capacity, and the maximum capillary height, but the permeability and the capillary rise rate are slower. the capillary rise height can also be influenced by the concentration of iron in the water [6,7] and the thermal conductivity [8].

Layering in the soil can affect both the downward infiltration and the upward capillary rise. Vertical infiltration in layered soils has been studied by many researchers [9–11]. All of these studies have reported that the infiltration in layered soils is complex because of the high nonlinearity of SWRC, hydraulic conductivity, various boundary and initial conditions, the textural contrast, and the hysteresis of SWRC, which increases the complexity further [12]. Compared with extensive research on the infiltration, the related reports about capillary rise in layered soils are relatively less, particularly on the water capillary rise process without evaporation. In a study of the capillary height in layered soil, the steady

state capillary rise was strongly influenced by the depth of the water table, and soil with a finer layer overlying a coarser layer, a linear relationship was observed between the thickness of the coarser layer and the critical groundwater depth, below which capillary water could not enter into the upper finer layer [13]. In a study of the water content profile, Shokri et al. [14] demonstrated that a capillary pressure jump caused by the air invading the interface between the finer and the coarser layers, and that will significantly modify the water distribution as compared to the homogeneous soil profile.

In the present study, laboratory column tests and numerical simulations were used to investigate the characteristics of the water capillary rise in layered soils. The results show that the soil suctions on the two sides of the interface, where is higher than the maximum capillary rise height of the coarser soil, are not same when water flow reaches the hydrostatic equilibrium condition.

2. Experiments

2.1. Material Properties

In this study, two types of commercially available sandy soil, called k-7 and k-8, were used. The grain size distributions for the two soils are shown in Figure 1. According to the standard (Japanese Geotechnical Society 0131 [15]), the k-7 soil is a sand (S-F) with a fine fraction (<0.075 mm) of around 10%, and the k-8 soil is a fine sand (SF), if British standard (EN ISO 14688-2 [16]) is applied, the k-7 soil can be classified as even-graded sand, and k-8 soil is a medium-graded sandy silt. The k-7 soil, and the k-8 soil have specific gravities of 2.67 and 2.69, respectively. Saturated hydraulic conductivity tests [17] were conducted on the k-7 soil by using the constant-head method and on the k-8 soil with the falling-head method. In constant-head test setup, the water supply at the inlet was adjusted to make the difference of head between the inlet and outlet remains constant during the test procedure. While in falling-head test setup, water from a standpipe flows through the soil and the water head varies with time. The saturated hydraulic conductivity of both soils was determined using the arithmetic mean of three tests at a dry density of 1.58 g/cm^3. The k-7 soil had a saturated hydraulic conductivity of 1.5×10^{-3} cm/s, and the value of the k-8 soil was 2.2×10^{-5} cm/s.

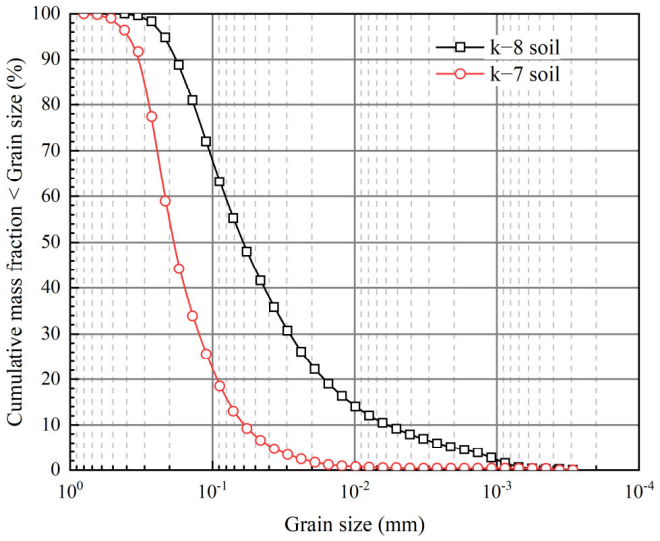

Figure 1. Grain size distributions for the soils used in the column capillary rise tests.

The soil water retention data of the soils were obtained during the wetting (sorption) process by using the two homogeneous soil columns, and then, the data points were fit to the van Genuchten model [18] by using the retention curve software (RETC [19]) to obtain

the soil water retention curves (Figure 2a). The volumetric water content, θ, and the suction head, h, were related as follows:

$$\theta = \theta_r + \frac{(\theta_s - \theta_r)}{\left[1 + (\alpha h)^n\right]^m} \quad (1)$$

where θ_s and θ_r indicate the saturated and the residual values of the volumetric water content, respectively. α, m, and n are the fitting parameters. The hydrologic parameters are given in Table 1. By adopting the hydraulic conductivity model proposed by Mualem [20], we predicted the hydraulic conductivity of a soil as a function of either the volumetric water content or the suction head by using these fitting parameters and the saturated hydraulic conductivity, k_{sat}. When the pore-connectivity parameter, l, was approximately 0.5 for many soils as originally proposed by Mualem [20], in terms of the suction head, the unsaturated hydraulic conductivity could be expressed as follows:

$$k(h) = k_{sat} \frac{\left\{1 - (\alpha h)^{nm}\left[1 + (\alpha h)^n\right]^{-m}\right\}^2}{\left[1 + (\alpha h)^n\right]^{\frac{m}{2}}} \quad (2)$$

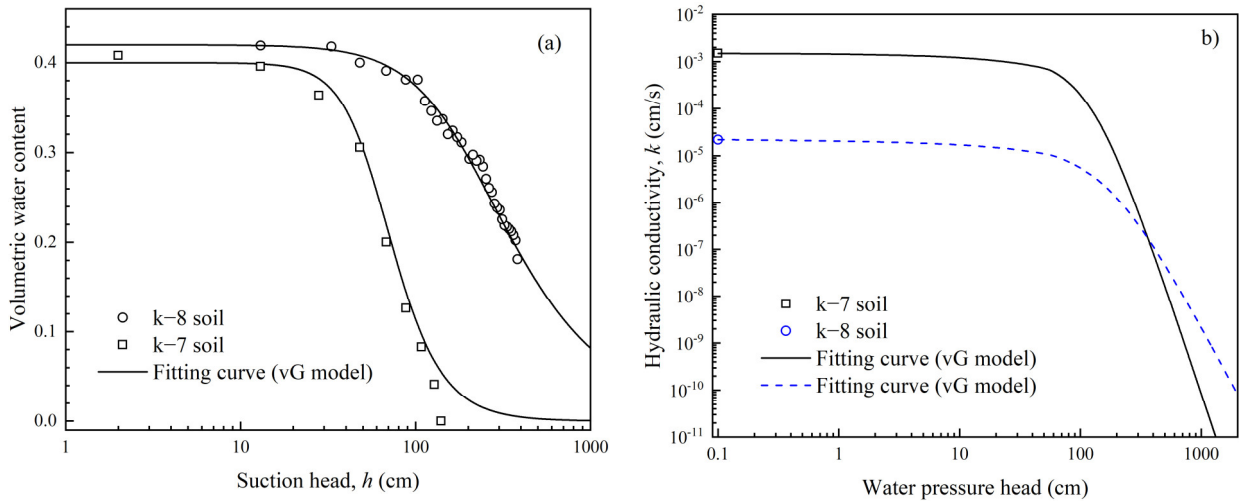

Figure 2. (**a**) Soil water retention curves (main wetting), and (**b**) unsaturated hydraulic conductivity curves for the k-7 and k-8 soils.

Table 1. Parameters applicable to the main wetting curve.

Soil	θ_s	θ_r	α (cm^{-1})	n	l
k-7	0.408	0	0.016	3.420	2.1
k-8	0.420	0.001	0.005	1.929	1

This equation cannot be solved unless the value of m − 1 + 1/n is an integer. The simplest case is for the value of 0, which leads to m = 1 − 1/n. Under this limit, the unsaturated hydraulic conductivities as a function of the suction head following a wetting path are as given in Figure 2b.

The soil water retention data were measured by gravimetric sampling (Figure 2a). As shown in the Figure 2a, under the same suction, the k-8 soil has a larger volumetric water content than that of the k-7 soil, which means thar the k-8 soil has the higher water retention capacity. The air entry value of the k-7 soil is about 30 kPa, for the k-8 soil, the value is about 100 kPa, at same time under this suction, the k-7 soil is nearly residual condition. As shown in the Figure 2b, the saturated hydraulic conductivity of the k-7 soil is 100 times over that of the k-8 soil; however, the value decays quickly. Conversely, the

hydraulic conductivity of the k-8 soil decrease slowly, therefore, the two curves intersect at the point where the suction is around 100 kPa.

2.2. Capillary Rise Experiments

The capillary rise experiments were conducted in the plexiglass column (Figure 3). Each column was composed with the same unit; the inner diameter and height were 100 mm and 200 mm, respectively, except at the position of the holes, where the time domain reflectometry (TDR) sensors were inserted. A rubber O-ring was placed in the groove, and the column units were connected to each other by bolts. The soils were first oven dried at 105 °C for 24 h (2017) and then placed into the columns. The soils were densified by vibration with a rubber hammer to achieve the target dry density of 1.58 g/cm^3 for both the k-7 soil and the k-8 soil. As shown in Figure 4, four layered soil cases were set up. A porous stone was placed at the bottom of the columns, and a lip with a 5-mm-diameter hole was fixed on the top of the columns. A constant 2-cm positive water head was maintained at the bottom of the columns during the entire test procedure. Each layered case adopted the stratified structure as a sandwich with a 20-cm-thick middle layer of the k-8 soil and a layer of the k-7 soil on the other two sides. The difference among these cases was the height where the k-8 soil was laid; the k-8 soil layer was laid from 20 cm, 60 cm, 100 cm, and 120 cm in columns A, B, C, and D, respectively. Twelve water content sensors (TDR (EC-5, Decagon Co., Ltd., Pullman, WA, USA)) were installed in each column. Two other homogeneous soil columns were set up as the controls by using the same preparation procedure as that of the other four columns. The height of the homogeneous k-7 soil column was 2 m and that for the homogeneous k-8 soil column was 3 m at first. However, the capillary water reached the top surface of the soil profile. To avoid the effect of evaporation, the homogeneous k-8 column was tested for the second time, and the height was 4 m. The data were automatically obtained by the data logger every 5 min. After 240 days, the final water contents were directly measured by disassembling the column and oven method along the center of the columns at the height where the TDR sensors were installed.



Figure 3. Setup of the capillary rise in the layered soil.

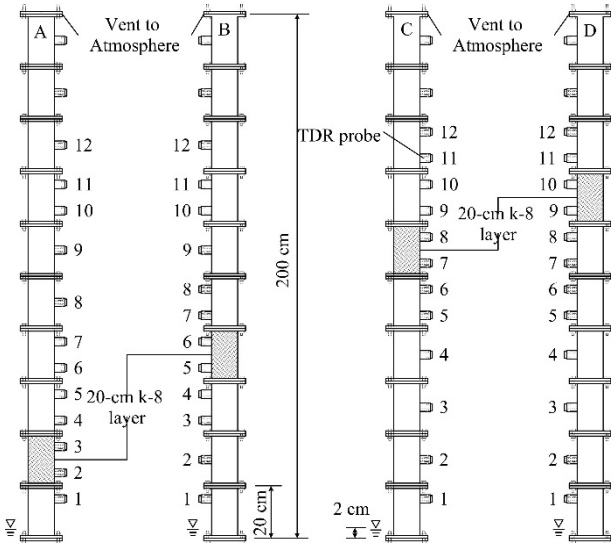

Figure 4. Schematic of the setup of the layered soil columns.

3. Numerical Simulation

The software Hydrus (2D/3D) [21] was used in this study. Based on the Richards equation [22], the numerical model was established following the experimental work, as described above. The upper boundary was set as the atmospheric condition without evaporation. The lower boundary was assigned to the condition of constant saturated water content. The entire finite element method (FEM) mesh was discretized uniformly except for the interface of the two soils, where a mesh refinement was added. The initial volumetric water content of the FEM column was set to 0.003, which was a little larger than the residual water content of both the soils. Next, 12 observation points were added to each FEM unit, at different elevations that were the same as the location of the TDR sensors in the physical model.

4. Results and Discussions

In all of the columns, the capillary water increased gradually with time (Figure 5a). The capillary water entered the finer interlayer (k-8 soil in this case) if it was laid lower than the maximum capillary height of the underlying coarser soil. The highest maximum capillary height, 153 cm, which was higher than the maximum capillary height of the homogeneous k-7 soil, was obtained in column D. However, in the other three columns, the maximum capillary height was the same as that of the homogeneous k-7 soil column. Therefore, once the water flowed into the finer soil, whether the maximum capillary height of layered soil was higher than that of the homogeneous soil depended on the height where the finer layer was laid. If the sum of the finer layer thickness and the coarser layer thickness (distance from the water level) was less than the maximum capillary height of the coarser layer, the maximum capillary height of layered soil was equal to that of the homogeneous coarser soil; otherwise, the former was larger.

The rate of capillary rise was different and not constant for each case. The capillary rate showed a power function relationship to the elapsed time; the corresponding regression equation is shown in Figure 5b. The tendency of the capillary rise rate in all of the layered cases was similar, which might be attributed to the fact that the thickness of the finer layer (20 cm) occupied a small portion of the total layered soil height, except in the case of column A. For column A, the finer soil layer was laid at a low position near the water level; it limited the water flow velocity because of its own lower hydraulic conductivity compared with that of the coarser soil in the same suction value.

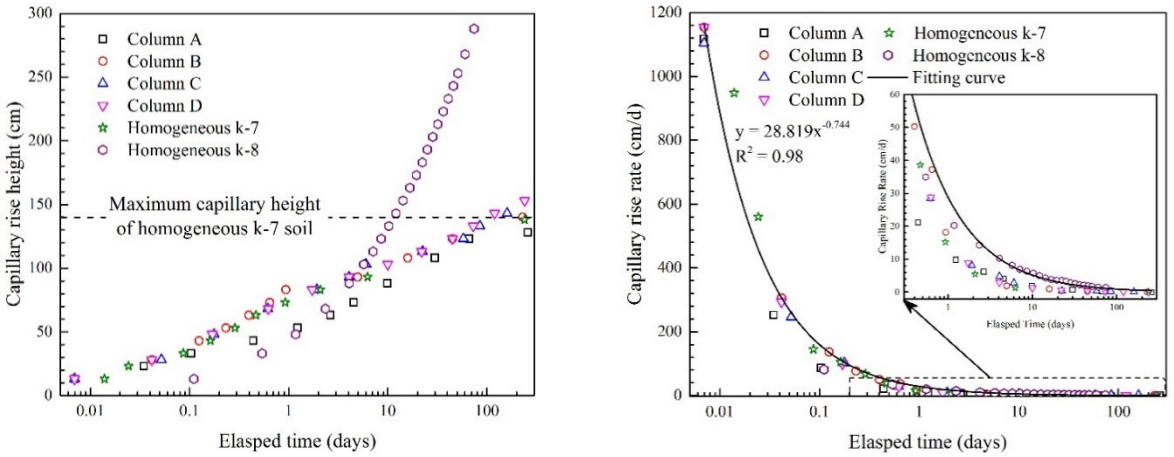

(**a**) Varying capillary rise height with elapsed time (**b**) Varying capillary rise rate with elapsed time

Figure 5. Comparison of the capillary rise height (**a**) and the rate (**b**) between the layered soil profile and the homogeneous soil profile.

Figure 6 shows the volumetric water content profiles of all of the six columns. The two solid curves are the water content profiles of the homogeneous k-7 and k-8 soil column, and the results of the other four layered cases are drawn as scatter plots. The water content value of the k-7 soil at the height greater than the maximum capillary height of the homogeneous k-7 soil was approximately equal to the residual water content. The water could be stored in the finer interlayer, and the amount of water was larger than that of the k-7 soil at the same height, but lower than that of the homogeneous k-8 soil at the same height. This result indicated a "gap" of the water content or suction between the interlayer k-8 soil and the homogeneous k-8 soil. According to the common view, the suction at the interface should be equal at two sides, therefore the water content at the two sides should be equal to the value of the homogeneous soil column at the height when the water flows reach at hydrostatic equilibrium condition. In other words, based on the observed water content, the suction of the layered soil might not be continuous because of the interface between the two types of soils due to the very different between the air entry values of the two kinds of soils.

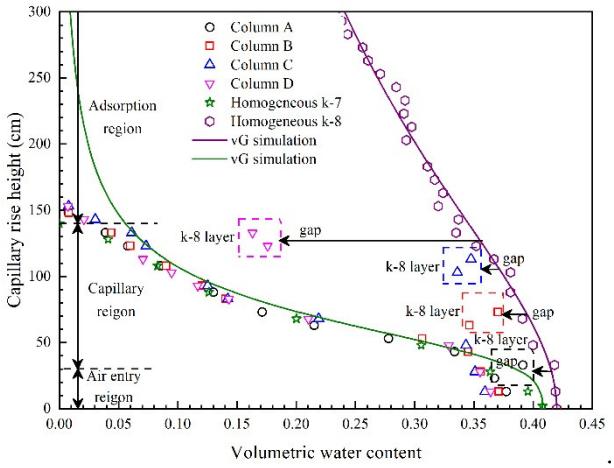

Figure 6. Water content distribution in the layered soil profile after the water capillary rise for 240 days.

As shown in Figure 7, generally, at most of the observed points, the numerical results were consistent with the test results. However, the simulated results of the finer soil layer (k-8 layer) were lower than that of the test results (Figure 7b). This implied that even if the

parameters in the simulation were same, it was difficult to ensure that the simulated results were consistent in all of the test cases. The effect of the interface played an important role in determining the characteristics of the water flow. Figure 7b shows that the measured volumetric water content increased with elapsed time. However, at observation point No. 4 (53 cm above the water level), the curve was not like the other observed results, which showed smooth increases; there was an obvious "slow down" process. The process started just before the water arrived at the adjacent higher observation point (No. 5, 63 cm above the water level) and ended when the volumetric water content of observation point No. 5 became steady. This result revealed that when the wetting front went through the interface between the coarser and the finer soil layer, the limit water from the lower section gave priority to the finer soil.

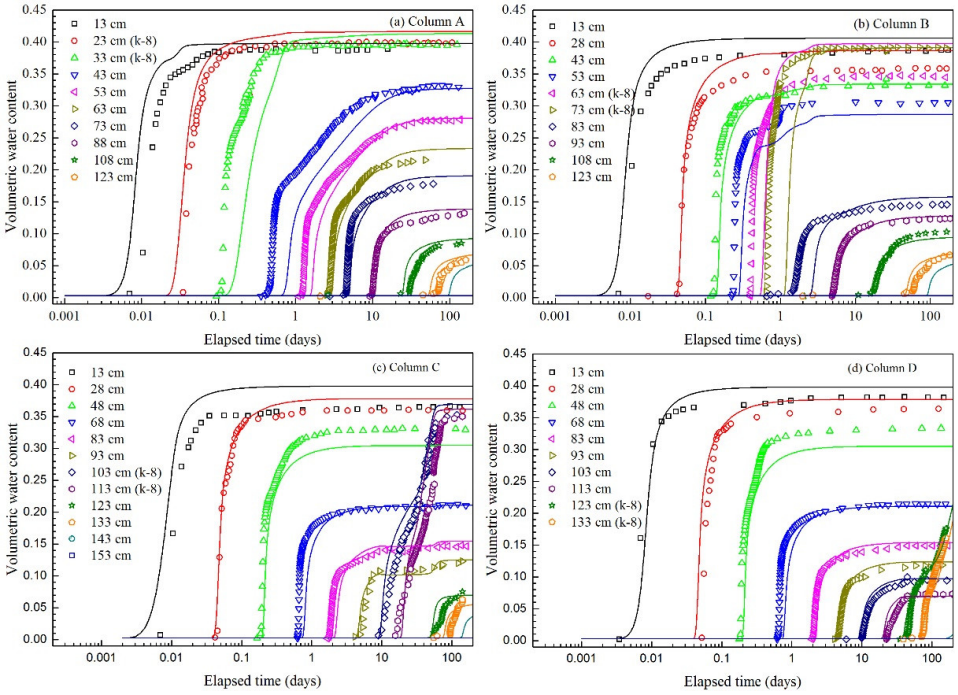

Figure 7. Comparison of the water content distribution in the layered soil profiles obtained by the test and the numerical simulation.

5. Conclusions

A series of capillary rise tests were conducted on soil columns of sand over fine sand over sand to investigate the effect of a relatively fine interlayer. In the layered soil, the water dynamics were affected not only by the interlayer properties and the thickness of the layers, but also by their spatial configuration. The soil water potential and the soil water distributions at equilibrium in the layered soil profile when the capillary water crossed the interlayer were different from those of the homogeneous soil column. The results showed that the water content was not continuous in the entire soil profile, and there were jumps at the coarser–finer soil and finer–coarser soil interfaces. The distribution of the matric suctions (calculated from the soil water retention curves) in this layered soil was similar to a profile without layering, but not the same. There was a small gap between these two wherever the finer layer in the middle was laid.

In the research work, the surface characteristics of soil particle such as the hydrophobicity was not taken into consideration. According to one of the reviewer's oping, the oven method can cause the possibility of hydrophobicity of the soil; however, the extent of the hydrophobicity should be studied in the further research. Although the column experiments had been conducted twice, only the successful case was presented in the paper, the other was failed due to the underestimation of the maximum capillary height of the

homogeneous k-8 soil. In engineering practice, using the coarser layer over finer layer can cut off the capillary water, which may take the salt rise to higher position in soil layer and cause the corrosion of concrete.

Author Contributions: Conceptualization, Z.L. and Z.Z.; Investigation, H.L. (Haitao Li) and H.S.; Writing—original draft preparation, Q.L.; Writing—review and editing, Z.Z.; Project administration, H.L. (Haiyan Liu); funding acquisition, Q.L. All authors have read and agreed to the published version of the manuscript.

Funding: This research was supported in part by Shandong Provincial Natural Science Foundation, China (ZR2021MD021).

Institutional Review Board Statement: Not applicable.

Informed Consent Statement: Not applicable.

Conflicts of Interest: The authors declare no conflict of interest.

References

1. Xu, X.; Sun, C.; Qu, Z.; Huang, Q.; Ramos, T.B.; Huang, G. Groundwater recharge and capillary rise in irrigated areas of the upper yellow river basin assessed by an agro-hydrological model. *Irrig. Drain.* **2016**, *64*, 587–599. [CrossRef]
2. Hird, R.; Bolton, M.D. Clarification of capillary rise in dry sand. *Eng. Geol.* **2017**, *230*, 77–83. [CrossRef]
3. Polansky, J.; Kaya, T. An experimental and numerical study of capillary rise with evaporation. *Int. J. Therm. Sci.* **2015**, *91*, 25–33. [CrossRef]
4. Liu, Q.; Yasufuku, N.; Miao, J.; Ren, J. An approach for quick estimation of maximum height of capillary rise. *Soils Found.* **2014**, *54*, 1241–1245. [CrossRef]
5. Wösten, J.H.M.; Pachepsky, Y.; Rawls, W. Pedotransfer functions: Bridging the gap between available basic soil data and missing soil hydraulic characteristics. *J. Hydrol.* **2001**, *251*, 123–150. [CrossRef]
6. Bai, B.; Jiang, S.; Liu, L.; Li, X.; Wu, H. The transport of silica powders and lead ions under unsteady flow and variable injection concentrations. *Powder Technol.* **2021**, *387*, 22–30. [CrossRef]
7. Bai, B.; Nie, Q.; Wu, H.; Hou, J. The attachment-detachment mechanism of ionic/nanoscale/microscale substances on quartz sand in water. *Powder Technol.* **2021**, *394*, 1158–1168. [CrossRef]
8. Bai, B.; Wang, Y.; Rao, D.; Bai, F. The effective thermal conductivity of unsaturated porous media deduced by pore-scale sph simulation. *Front. Earth Sci.* **2022**, *10*, 943853. [CrossRef]
9. Zhu, J.; Mohanty, B.P. Analytical solutions for steady state vertical infiltration. *Water Resour. Res.* **2002**, *38*, 20-21–20-25. [CrossRef]
10. Huang, M.B.; Barbour, S.; Elshorbagy, A.; Zettl, J.; Si, B. Infiltration and drainage processes in multi-layered coarse soils. *Can. J. Soil Sci.* **2011**, *91*, 169–183. [CrossRef]
11. Ma, Y.; Feng, S.; Zhan, H.; Liu, X.; Su, D.; Kang, S.; Song, X. Water infiltration in layered soils with air entrapment: Modified green-ampt model and experimental validation. *J. Hydrol. Eng.* **2011**, *16*, 628–638. [CrossRef]
12. Serrano, S.E. Modeling infiltration in hysteretic soils. *Adv. Water Resour.* **1990**, *13*, 12–23. [CrossRef]
13. Bloemen, G. Calculation of steady state capillary rise from the groundwater table in multi-layered soil profiles. *Z. Pflanz. Bodenkd.* **1980**, *143*, 701–719. [CrossRef]
14. Shokri, N.; Lehmann, P.; Or, D. Evaporation from layered porous media. *J. Geophys. Res. Solid Earth* **2010**, *115*, 258–273. [CrossRef]
15. Japanese Geotechnical Society. *Laboratory Testing Standards of Geomaterials*; Japanese Geotechnical Society: Tokyo, Japan, 2017.
16. *BS EN ISO 14688-2*; Geotechnical Investigation and Testing Identification and Classification of Soil, Part 2: Principles for a Classification. British Standards Institution: London, UK, 2004.
17. Amer, A.M.; Awad, A. Permeability of cohesionless soils. *J. Geotech. Eng. Div. ASCE* **1974**, *100*, 1309–1316. [CrossRef]
18. Van Genuchten, M.T. A closed-form equation for predicting the hydraulic conductivity of unsaturated soils. *Soil Sci. Soc. Am. J.* **1980**, *44*, 892–898. [CrossRef]
19. Van Genuchten, M.T.; Simunek, J.; Leij, F.; Sejna, M. *The Retc Code for Quantifying the Hydraulic Functions of Unsaturated Soils, Version 1.0.*; Epa Report 600/2-91/065; U.S. Salinity Laboratory, USDA, ARS: Riverside, CA, USA, 1991.
20. Mualem, Y. A new model for predicting the hydraulic conductivity of unsaturated porous media. *Water Resour. Res.* **1976**, *12*, 593–622. [CrossRef]
21. Šimůnek, J.; van Genuchten, M.; Šejna, M. Development and applications of the hydrus and stanmod software packages and related codes. *Vadose Zone J.* **2008**, *7*, 587–600. [CrossRef]
22. Richards, L.A. Capillary conduction of liquids through porous mediums. *Physics* **1931**, *1*, 318–333. [CrossRef]

Disclaimer/Publisher's Note: The statements, opinions and data contained in all publications are solely those of the individual author(s) and contributor(s) and not of MDPI and/or the editor(s). MDPI and/or the editor(s) disclaim responsibility for any injury to people or property resulting from any ideas, methods, instructions or products referred to in the content.